Liu *et al. BMC Cancer* (2025) 25:387
https://doi.org/10.1186/s12885-025-13576-4

BMC Cancer

RESEARCH Open Access

Causal relationship between immune cell signatures and colorectal cancer: a bi-directional, two-sample mendelian randomization study

Ruizhi Liu[1†], Liansha Tang[2†], Yunjia Liu[3], Handan Hu[4] and Jiyan Liu[2*]

Abstract

Background Prior studies have demonstrated the association between immune cells and colorectal cancer (CRC). However, the causal link to specific immunophenotypes is limited. This study intends to elucidate the causal relationship of immune cell signatures on CRC.

Methods We performed a bi-directional and two-sample mendelian randomization (MR) study, utilizing GWAS summary data of 731 immune cell traits ($n=3,757$) and CRC statistics ($n=470,002$). The primary MR methodology was inverse-variance weighted (IVW) method. Furthermore, heterogeneity was evaluated by Cochran's Q test. MR-PRESSO and MR-Egger were employed to assess horizontal and vertical pleiotropy respectively. Sensitivity analysis and FDR correction were conducted in our results. These results were validated in both the UK Biobank and FinnGen cohorts. We also extracted transcriptomic data of CRC and adjacent non-tumor tissues from TCGA, and used CIBERSORT to compare the infiltration patterns of 22 immune cell panels between normal tissues and the tumor microenvironment (TME).

Results Our study indicated nine immune cell signatures had significant causality with the risk of CRC after sensitivity analysis and FDR correction. The positive results covered four panels: B cell, CD8 + T cell, Treg, and monocyte. IgD- CD38br and IgD + CD38br B cell, CD8dim and CD28 + CD45RA- CD8dim T cell, and CD14 on CD14 + CD16- monocyte were the protective factors of CRC. However, CD39 + resting Treg, CX3CR1 on CD14- CD16 + monocyte, FSC-A on HLA DR + T cell, and BAFF-R on B cell increased the risk of CRC. The results were validated in the UK Biobank data and FinnGen cohorts. The data from the TCGA database also confirmed the infiltration of B cell, CD8 + T cell, Treg, and monocyte panels in the TME.

Conclusion This study highlights the causal link between specific immune cell phenotypes and CRC, providing valuable insights into the immune microenvironment's role in CRC. The validation of our findings using large-

†Ruizhi Liu and Liansha Tang contributed equally to this work.

*Correspondence:
Jiyan Liu
liujiyan1972@163.com

Full list of author information is available at the end of the article

scale datasets (UK Biobank, FinnGen) and TCGA underscores the robustness of our results, offering new potential therapeutic targets for CRC treatment.

Keywords Immune cell, Colorectal cancer, MR analysis, Treg, Tumor microenvironment

Introduction

Colorectal cancer (CRC) is the third leading cancer in the United States, with about 152,810 estimated new cases and 53,010 deaths in 2024 [1]. Furthermore, it has been reported that the incidence of CRC in younger individuals (under 50 years old) is alarmingly on the rise [2]. Hull et al. suggested that half of CRC cases could be preventable [3]. Therefore, pinpointing new risk factors could greatly benefit the future diagnosis and management of CRC.

CRC is propelled by the accumulation of gene alterations and epigenetic modifications. Based on the heterogeneity of immune response, CRC is divided into two genetically different subtypes, mismatch repair-proficient (MMRp) and mismatch repair-deficient (MMRd) [4]. MMRp CRC has a lower mutation burden and shows no response to immunotherapy, while MMRd CRC with higher mutation burden is often infiltrated with cytotoxic (CD8) T cell and demonstrates a notable response rate to immunotherapy [5, 6].

There is a strong and close association between tumor microenvironment (TME) and CRC [7, 8]. In the TME, immune cells can be categorized into immune-activating cells (e.g., CD8 + T cells, NK cells), immune-suppressive cells (e.g., Tregs), and cells with dual functions, such as B cells. The dynamic balance among these cells dictates the immune system's ability to eliminate tumors. CD8 + T cells play a pivotal role in immune surveillance, directly or indirectly killing target cells to exert anti-tumor effects [9]. After recognizing and eliminating tumor cells, some CD8 + T cells enter a memory state, enabling rapid reactivation and a more robust immune response upon subsequent antigen exposure. The infiltration of CD8 + and memory (CD45RO) T cells was linked to favorable prognosis and low recurrence risk in CRC patients [10]. NK cells regulate anti-tumor immunity by secreting pro-inflammatory cytokines, such as tumor necrosis factor-α (TNF-α) and interferon-γ (IFN-γ), which inhibit tumor cell proliferation and angiogenesis [11]. Higher NK cell proportions in tumor tissue, metastatic liver lesions, and peripheral blood, suggest superior clinical outcomes in CRC patients [12].

On the contrary, regulatory T cells (Tregs), by secreting immunosuppressive cytokines such as TGF-β and IL-10, inhibit the inflammatory response induced by effector T cells, thereby helping tumors evade immune surveillance and promoting immune escape [13]. However, the impact of Tregs on CRC prognosis remains inconclusive [14, 15], possibly due to the presence of Treg subsets with similar phenotypes but distinct functions. B cells induce the formation of tertiary lymphoid structures (TLS) in non-lymphoid tissues by secreting lymphotoxin (LT)-α1β2, which is essential for immune regulation, particularly in orchestrating local immune responses and enhancing memory T cell responses. In addition, B cells can produce immunosuppressive cytokines IL-35 and IL-10, thereby facilitating tumor progression [16]. Zhang et al. suggested that B cells exerted a positive anti-tumor effect in the CRC [17], while Bindea et al. found that B cells played dual roles in CRC progression and recurrence [18]. The effects of various immune cells on the development of CRC are complex and differ sharply between individual tumors [19].

Although observational studies have established associations between immune phenotypes and CRC, confounding factors [20] such as diet, lifestyle, and environmental exposures, as well as reverse causality, limit causal inference. Mendelian Randomization (MR) overcomes these limitations by using genetic variants as instrumental variables (IVs) to infer causality. Rooted in Mendel's laws of inheritance, MR leverages the random segregation of alleles to mimic the randomization process of controlled trials, minimizing reverse causation and confounding bias [21].

MR has been widely applied in cancer research to identify causal links between cancer-related risk factors, including lifestyle, metabolites, and cancer outcomes. Immune phenotypes are particularly integral for CRC, given their critical yet complex roles in tumor development and progression. Using SNPs related to immune traits as IVs, MR provides a powerful tool to assess the causal impact of these traits on CRC risk. We conducted a two-sample MR analysis to explore the causality between 731 immune phenotypes and CRC. This study aims to clarify how immune cells influence CRC pathogenesis, enhance insights into TME interactions, and inform innovative immunotherapies.

Materials and methods

Study design

A two-sample MR analysis was utilized to determine the causal effects of 731 immune cell signatures on the risk of CRC. The instrumental variables (IVs) are represented by genetic variations. The eligible IVs should fulfill these three conditions. Firstly, genetic variations are directly associated with exposure. Secondly, they should not be related to potential confounders. At last, these IVs exclusively influence the outcome via the exposure,

with no impact stemming from alternate pathways. This study used publicly available data, which were previously approved by the relevant ethics committees, and therefore no additional informed consent was required.

GWAS data sources for exposure and outcomes

Public GWAS data for immunological traits were obtained with accession numbers GCST0001391 to GCST0002121 [22]. This research comprised 731 immune cell phenotypes, containing 32 morphological parameters (MP), 389 median fluorescence intensities (MFI) signifying surface antigen levels, 192 relative cell counts (RC), and 118 absolute cell counts (AC). All 731 immunological traits were included in the analysis to maintain comprehensiveness and enable an unbiased exploration of their relevance to CRC, with no additional filtering applied.

The RC, AC and MFI features encompass B cell, monocyte, myeloid cell, Treg, maturation stages of T cell, TBNK (T cell, B cell, NK cell), conventional dendritic cell (cDC). The MP features cover TBNK and cDC panels. RC and AC are closely linked to the immune system's response to tumors. Increased numbers of immune-activating cells, such as CD8 + T cells and NK cells, typically indicate effective anti-tumor immunity, while higher levels of immunosuppressive cells, like Tregs and myeloid-derived suppressor cells (MDSCs), may promote tumor progression. MFI reflects surface antigen expression, such as CD4/CD8 on T cells and CD19/CD20 on B cells, indicating cell phenotypes and functional states. Changes in these antigens may reflect the functional status of tumor-infiltrating lymphocytes (TILs). MP describes immune cell size, shape, and internal complexity, including forward and side scatter characteristics. In the CRC microenvironment, immune cells may exhibit unique morphological traits indicative of functional changes, such as the enlargement of activated T or B cells. MP features of TBNK and cDC cells may be associated with tumor infiltration, antigen-presenting capacity, and functional states.

Drawing on data from 3,757 European individuals, this study revealed associations across more than 22 million SNP genotypes, adjusting for confounders like age and sex, and utilized a Sardinian sequence-based reference panel [23]. Genotype quality control was rigorously performed prior to the exposure GWAS analysis, including the removal of individuals and SNPs with high missing rates. Imputation quality scores (RSQR) were also used, with SNPs having an RSQR over 0.3 (MAF ≥ 1%) or over 0.6 (MAF < 1%) selected for subsequent analysis. These quality control steps effectively minimized noise caused by missing or low-quality imputed data.

GWAS data for colorectal cancer (CRC) were obtained from three sources: European participants from a cross-population study in the IEU Open GWAS database [24], used as the outcome data in the primary analysis (training set), and two studies from the UK Biobank [25] and the FinnGen cohort (https://www.finngen.fi/en, ID: C3_COLORECTAL_EXALLC), used as the validation sets for subsequent analyses. The cross-population study included 470,002 European participants (6,581 cases and 463,421 controls), identifying about 5,000 novel genomic loci and adjusting age and sex. The data from the UK Biobank covered 11,738,639 SNPs, consisting of 5,657 CRC cases and 372,016 controls. The FinnGen database involved 6,847 CRC patients and 314,193 controls.

Selection of instrumental variables (IVs)

The IVs should satisfy the following criteria: (1) The significance threshold for IVs was set at $p < 5 \times 10^{-6}$ [26]. (2) SNPs with $r^2 < 0.001$ within 10,000 kb are removed to address linkage disequilibrium (LD), ensuring allele frequencies between loci are not correlated. (3) F-statistics assess the strength of IVs, with higher values indicating stronger predictive power. Only IVs with an F-statistic > 10 were considered valid and reliable, helping to avoid weak instrument bias that could affect the MR results [27, 28]. (4) SNPs for analysis were selected using the outcome ID. SNPs with a P-value less than 5×10^{-8} (indicating significant association with the outcome) were excluded, as they may directly affect the outcome. This criterion ensures that the selected SNPs influence the outcome only through exposure, avoiding direct associations with the outcome. (5) MR analysis required SNP effects on outcomes due solely to exposure to one allele, aligning exposure and outcome SNPs for consistent effect estimates. SNPs with intermediate EAFs (> 0.42) or incompatible alleles were omitted. (6) The PhenoScanner V2 was used to eliminate SNPs related to possible confounders.

Two-sample MR analysis

During the data integration process, we used GRCh37 as a unified reference genome version to align genotype data from different GWAS sources to the same coordinate system, thereby eliminating potential biases due to differences in reference genome versions. For the exposure and outcome data in the GWAS, several standardization procedures were applied to ensure data consistency. For example, immune cell measurements were standardized by daily calibration of the FACS CantoII analyzers and regular validation of cell counts. In the selection signal analysis, some factors, such as MAF, local recombination rate, and background selection pressure, were standardized to ensure consistent comparisons of variants. These standardization measures ensured the reliability of the GWAS data in the MR analysis and improved the accuracy of the results. In addition, age and

sex have already been adequately adjusted in the exposure and outcome GWAS data, so we did not repeat these adjustments in the subsequent MR analysis. Multiple MR methods, containing inverse variance weighting (IVW), MR-Egger, weighted median, weighted mode, and simple mode, were in this study. Our primary MR analysis utilized the IVW method, which combined individual SNP Wald ratios via meta-analysis. It assumed IVs affected outcomes only through the exposure, ensuring unbiased causal estimates by excluding horizontal pleiotropy [29].

Sensitivity analysis

We conducted a sensitivity analysis to evaluate possible heterogeneity and pleiotropy. Cochran's Q test used random-effects IVW for significant variation among genetic IVs ($p < 0.05$) for heterogeneity [30]. MR-PRESSO addressed outliers and horizontal pleiotropy, while MR-Egger's intercept evaluated vertical pleiotropy [31]. Leave-one-out analysis assessed the influence of individual SNPs on the overall findings. Scatter and funnel plots verified the results' integrity and homogeneity, respectively. We corrected p-values for multiple examinations using FDR (Benjamini-Hochberg method), considering < 0.05 as significant for causality. Reverse causality between immune cell phenotypes and CRC was investigated using the same analytical approach.

Immune cell infiltration in TCGA

The transcriptome profiles of CRC were obtained from the Genomic Data Commons Data Portal of TCGA (https://portal.gdc.cancer.gov/). The gene expression data included 695 samples, consisting of 51 adjacent non-tumorous tissues and 644 CRC tissues.

Immune cell infiltration was quantified using the CIBERSORT algorithm [32], which utilizes a gene expression matrix of 547 marker genes to estimate the relative abundance of immune cell types. LM22 matrix, which defines 22 immune cell subtypes, was obtained from the CIBERSORT web portal (http://cibersort.stanford.edu/). These subtypes include eosinophils, activated NK cells, resting NK cells, M0-M2 macrophages, resting mast cells, activated mast cells, memory B cells, naive B cells, neutrophils, monocytes, activated dendritic cells, resting dendritic cells, plasma cells, and seven T cell subsets. Improving the precision of the algorithm, we calculated the root mean square error (RMSE) and CIBERSORT p-values for each sample. The algorithm was executed with the default signature matrix and 1000 permutations. Samples with a CIBERSORT p-value less than 0.05 were retained for further analysis.

The immune cell proportions in CRC and normal samples were analyzed using the CIBERSORT algorithm. We performed the Wilcoxon rank-sum test to compare immune cell infiltration between tumor and normal tissues. All analysis were conducted in R 4.3.2 software.

Results

Identification of SNPs

The study flowchart is shown in Fig. 1. All SNPS associated with immune cells were shown in Supplementary Table 1. Supplementary Table 2 showed eligible SNPs for a two-sample MR analysis based on specific screening criteria. Despite using Phenoscanner to search for CRC-related SNPs, we found no significant connections between these SNPs and potential confounders.

The causal effect of immune cell phenotypes on colorectal cancer

The causal effects of immune cell traits on CRC were shown in Fig. 2. We utilized IVW as the main method to identify the causality between immune immunophenotypes and CRC. The effect estimates from all five MR methods consistent in direction. The results showed nine immune immunophenotypes were positively linked to the risk of CRC (Fig. 3 and Supplementary Table 3), including B cell, Treg, CD8 + T cell, and monocyte panel. We found IgD- CD38br AC (OR = 0.933, 95% CI: 0.882 to 0.987, $P = 0.016$), IgD + CD38br% lymphocyte (OR = 0.940, 95%CI: 0.889–0.994, $P = 0.031$), CD8dim% lymphocyte (OR = 0.936, 95%CI: 0.876-1.000, $P = 0.048$), CD28 + CD45RA- CD8dim%CD8dim (OR = 0.963, 95%CI: 0.930–0.998, $P = 0.036$), and CD14 on CD14 + CD16- monocyte (OR = 0.931, 95%CI:0.885–0.980, $P = 0.006$) could significantly decrease the risk of CRC. However, CD39 + resting Treg AC (OR = 1.035, 95%CI:1.003–1.068, $P = 0.031$), CX3CR1 on CD14-CD16 + monocyte (OR = 1.052, 95%CI:1.011–1.094, $P = 0.011$), BAFF-R on B cell (OR = 1.028, 95%CI: 1.001–1.055, $P = 0.039$), and FSC-A on HLA DR + T cell (OR = 1.069, 95%CI: 1.003–1.139, $P = 0.04$) were the risk factor for CRC. P value was still significant (< 0.05) after FDR correction, suggesting the robustness of our results.

These results were detected significant heterogeneity by the Cochran Q test (Table 1). Our sensitivity analysis, including MR-Egger regression and MR-PRESSO analysis, did not find genetic pleiotropy bias (Table 1). The scatter plots (Fig. 4), leave one-out analysis (Fig. 5), and funnel plots (Fig. 6) for the relationship were presented.

The causal effect of colorectal cancer on immune cell phenotypes

Reverse MR was conducted between CRC and immunophenotypes (Supplementary Table 4). We did not find the positive relationship between CRC and immunophenotypes. The P-values of the MR method using IVM were all greater than 0.05, indicating no significant reverse causality.

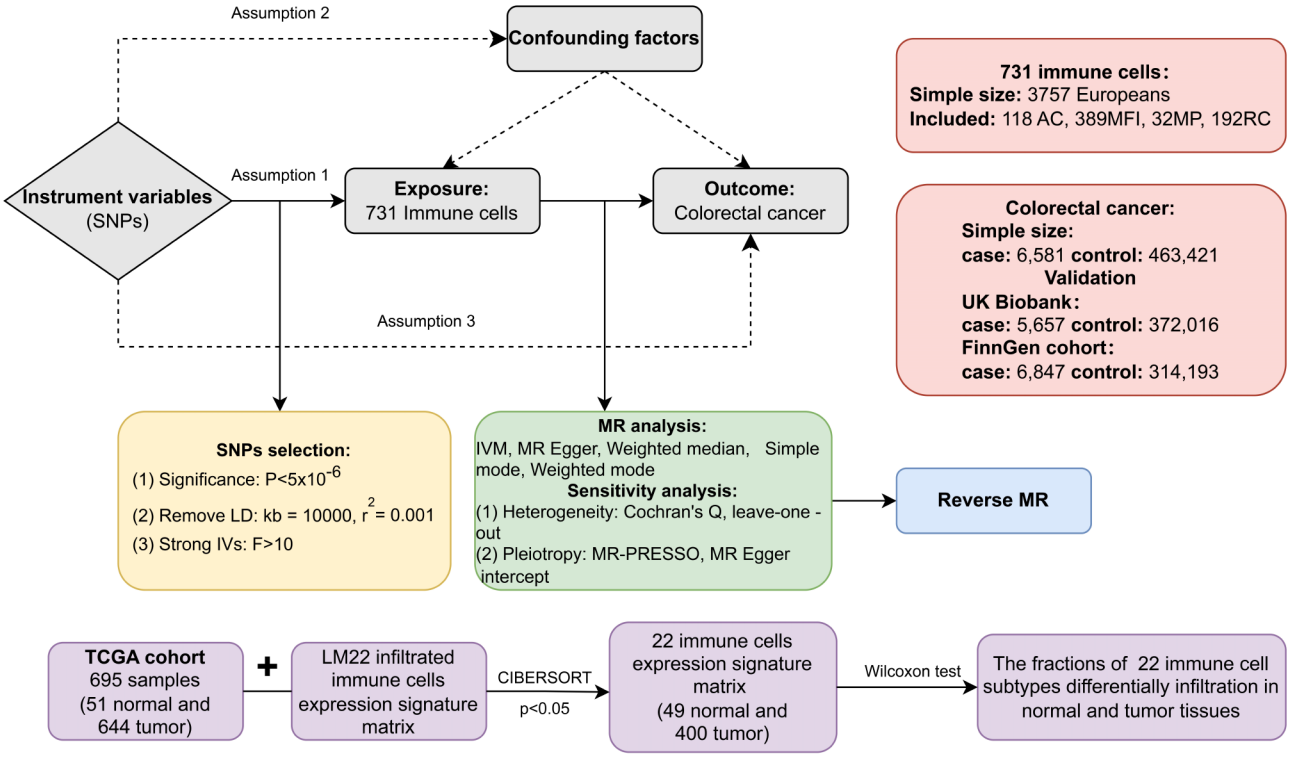

Fig. 1 Overview of MR design

Data validation in UK Biobank and Finngen cohort

The SNPs from the UK Biobank and FinnGen cohorts used for MR analysis were shown in Supplementary Tables 5 and 6. In the UK Biobank, CD14 on CD14 + CD16 + monocyte (OR = 1.001, 95%CI: 1.000-1.003, $P = 0.025$), CD28 + CD45RA- CD8dim %CD8dim (OR = 0.999, 95%CI: 0.999-1.000, $P = 0.033$), resting Treg % CD4 Treg (OR = 1.001, 95%CI:1.000-1.001, $P = 0.036$), and resting Treg %CD4 (OR = 1.001, 95%CI: 1.000-1.001, $P = 0.008$) were validated (Supplementary Table 7). The results of CD8dim %leukocyte (OR = 0.912, 95%CI: 0.839–0.992, $P = 0.032$) and FSC-A on HLA DR + T cell (OR = 1.128, 95%CI: 1.018–1.251, $P = 0.022$) were identified in the FinnGen database (Supplementary Table 8). The P-values of the MR method using IVM remained significant (< 0.05) after FDR correction. Reverse MR did not find the positive relationship between CRC and immunophenotypes in either database.

Comparison of immune cell types in tumor and normal tissues in the TCGA

After filtering with CIBERSORT $p < 0.05$, the proportion of immune cell infiltration between adjacent normal and tumor tissues in the TCGA cohort was shown in Fig. 7A and Supplementary Table 9, containing 49 adjacent normal tissues and 400 CRC tissues. Figure 2B-C depicted the differences in immune cell infiltration between these two tissues. The proportions of naive B cells, CD8 + T cells, Tregs, and monocytes in the CRC microenvironment showed consistent trends with the Mendelian results. CD8 + T cells, naive B cells, and monocytes infiltrated more in CRC tissues, while Tregs presented the higher fraction in CRC tissues. Compared with normal tissues, CRC samples exhibited a significantly higher percentage of M0-M1 macrophages, activated mast cells, resting NK cells, follicular helper T cells, and neutrophils. The correlations of immune cells in CRC tissues were shown in Fig. 2D. Follicular helper T cell, M1 macrophages and activated CD4 + memory T cells showed the most significant positive correlation with CD8 + T cells. Activated CD4 + memory cells presented the highest negative correlation with Tregs.

Discussion

Our research utilized two-sample and bi-directional MR analysis to identify the causality between immune cell signatures and the risk of CRC, combined with public GWAS data. We found four immune cell panels (CD8 + T cells, B cells, Tregs, and monocytes) were significantly associated with CRC, as identified in the TCGA immune cell infiltration analysis. These included two CD8 + T cell subsets (CD8dim and CD28 + CD45RA- CD8dim T cells), two B cell subsets (IgD- CD38br and IgD + CD38br B cells), one Treg subset (CD39 + resting Tregs), one B cell surface marker (BAFF-R), and two monocyte surface

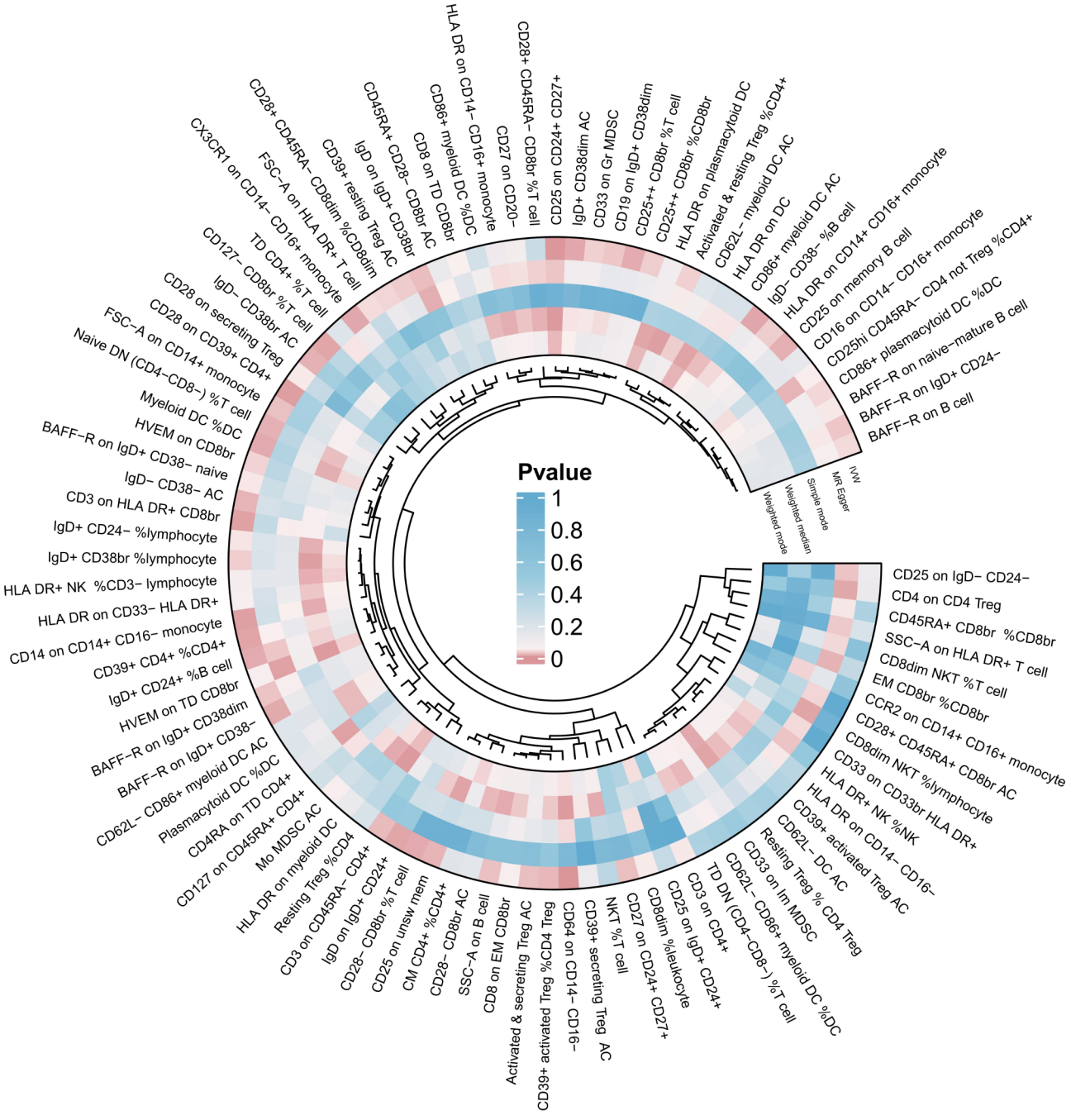

Fig. 2 The circular heatmap illustrates the clustering of immune cell subsets and their association with CRC. The inner dendrogram groups immune cell subsets, while the outer heatmap displays p-values from various statistical analyses, with red indicating stronger associations (lower p-values) and blue indicating weaker associations (higher p-values). Immune cell subsets, including CD8 + T cells, B cells, Tregs, and monocytes, showed significant associations with CRC. Statistical methods of MR are represented in the outer rings

markers (CD14 and CX3CR1), along with FSC-A on HLA DR + T cells.

Two CD8 + T cells and B cells, as well as CD14 on monocyte were the protective factors for CRC, while BAFF-R on B cell, CD39 + resting Treg, CX3CR1 on monocyte and FSC-A on HLA DR + T cell were the risk factors. Furthermore, the reverse MR results were not valid. The UK Biobank CRC data validated CD14 on monocytes, resting Treg, and CD28 + CD45RA- CD8dim %CD8dim T cell. The FinnGen data confirmed the causal relationship between CD8dim %leukocyte, FSC-A on HLA DR + T cells, and CRC.

Exposure	Outcome	nsnp	Method	pval	OR(95% CI)	revPvalue	pFDR
IgD− CD38br AC	Colorectal Cancer	9	MR Egger	0.442	0.957 (0.862 to 1.063)		
		9	Weighted median	0.108	0.941 (0.873 to 1.013)		
		9	Inverse variance weighted	**0.016**	0.933 (0.882 to 0.987)	0.214	**0.038**
		9	Simple mode	0.537	0.966 (0.870 to 1.073)		
		9	Weighted mode	0.442	0.955 (0.856 to 1.067)		
IgD+ CD38br %lymphocyte	Colorectal Cancer	11	MR Egger	0.203	0.924 (0.826 to 1.034)		
		11	Weighted median	**0.005**	0.895 (0.827 to 0.968)		
		11	Inverse variance weighted	**0.031**	0.940 (0.889 to 0.994)	0.618	**0.043**
		11	Simple mode	0.142	0.894 (0.780 to 1.026)		
		11	Weighted mode	**0.040**	0.888 (0.804 to 0.980)		
BAFF−R on B cell	Colorectal Cancer	13	MR Egger	0.063	1.040 (1.002 to 1.080)		
		13	Weighted median	0.156	1.021 (0.992 to 1.050)		
		13	Inverse variance weighted	**0.039**	1.028 (1.001 to 1.055)	0.056	**0.047**
		13	Simple mode	0.422	1.023 (0.970 to 1.079)		
		13	Weighted mode	0.160	1.021 (0.994 to 1.050)		
CD14 on CD14+ CD16− monocyte	Colorectal Cancer	10	MR Egger	0.245	0.944 (0.863 to 1.033)		
		10	Weighted median	**0.013**	0.921 (0.862 to 0.983)		
		10	Inverse variance weighted	**0.006**	0.931 (0.885 to 0.980)	0.922	**0.038**
		10	Simple mode	0.051	0.912 (0.842 to 0.988)		
		10	Weighted mode	0.062	0.923 (0.858 to 0.994)		
CX3CR1 on CD14− CD16+ monocyte	Colorectal Cancer	11	MR Egger	0.106	1.057 (0.995 to 1.124)		
		11	Weighted median	0.476	1.020 (0.965 to 1.079)		
		11	Inverse variance weighted	**0.011**	1.052 (1.011 to 1.094)	0.175	**0.038**
		11	Simple mode	0.297	1.045 (0.966 to 1.131)		
		11	Weighted mode	0.419	1.026 (0.966 to 1.090)		
CD8dim %leukocyte	Colorectal Cancer	9	MR Egger	0.672	0.946 (0.739 to 1.211)		
		9	Weighted median	0.250	0.951 (0.873 to 1.036)		
		9	Inverse variance weighted	**0.048**	0.936 (0.876 to 1.000)	0.537	**0.049**
		9	Simple mode	**0.042**	0.819 (0.696 to 0.963)		
		9	Weighted mode	0.386	0.960 (0.880 to 1.047)		
CD28+ CD45RA− CD8dim %CD8dim	Colorectal Cancer	13	MR Egger	0.119	0.961 (0.918 to 1.006)		
		13	Weighted median	0.304	0.976 (0.931 to 1.022)		
		13	Inverse variance weighted	**0.036**	0.963 (0.930 to 0.998)	0.533	**0.045**
		13	Simple mode	0.708	0.987 (0.924 to 1.055)		
		13	Weighted mode	0.274	0.975 (0.933 to 1.018)		
FSC−A on HLA DR+ T cell	Colorectal Cancer	8	MR Egger	0.300	1.062 (0.957 to 1.180)		
		8	Weighted median	0.360	1.041 (0.955 to 1.134)		
		8	Inverse variance weighted	**0.040**	1.069 (1.003 to 1.139)	0.062	**0.047**
		8	Simple mode	0.439	1.052 (0.931 to 1.189)		
		8	Weighted mode	0.379	1.039 (0.959 to 1.125)		
CD39+ resting Treg AC	Colorectal Cancer	21	MR Egger	0.147	1.034 (0.990 to 1.081)		
		21	Weighted median	0.445	1.017 (0.973 to 1.063)		
		21	Inverse variance weighted	**0.031**	1.035 (1.003 to 1.068)	0.56	**0.043**
		21	Simple mode	0.618	1.018 (0.950 to 1.092)		
		21	Weighted mode	0.216	1.031 (0.984 to 1.080)		

Fig. 3 The forest plot derived from five MR methods demonstrates the impact of immune cell characteristics on CRC. Utilizing the IVW method as the main result, a P-value less than 0.05 is deemed indicative of an association between the immune cell phenotype and the risk of CRC

CD8 + T cell

CD8 + T cells are classified into CD8br and CD8dim subsets based on CD8 expression levels, but their functional roles remain uncertain. Our results demonstrated that CD8dim T cells were associated with a reduced risk of colorectal cancer. A previous study reported that CD8dim T cells mediated cytotoxic responses by releasing granzyme B [33]. Compared to CD8br T cells, CD8dim T cells exhibit higher levels of CD56 expression, resembling NK-like functions. CD28, a co-stimulatory molecule on T cells, enhances glycolysis, providing the energy required for growth and proliferation [34]. In CD8 + T cells, CD28 promotes cytokine production, survival, migration, and anti-tumor activity. CD45RA, typically expressed on naïve or unactivated T cells, is absent on CD28 + CD45RA- CD8dim T cells, indicating they are likely memory T cells that have undergone prior activation [35]. These cells, classified as effector memory T cells (T_EM), are capable of rapid responses upon antigen re-exposure, maintaining immune surveillance with readiness to counter infections or stimuli [36]. Consistent with our findings, CD28 + CD45RA- CD8dim T cells acted as protective factors against CRC, validated in the UK Biobank dataset. Further exploration of immune cell subset specialization will provide critical insights into the tumor immune microenvironment and guide the optimization of immunotherapy.

Treg

Tregs are categorized into three groups by their surface markers: activated Tregs (aTregs) (CD45RA-FoxP3^{hi}), resting Tregs (rTregs) (CD45RA + FoxP3^{lo}), and secreting

Table 1 Sensitivity analysis of immune cell characteristics and colorectal cancer in MR analysis

Panel	Exposure	Number of SNPs	MR Egger regression		Heterogeneity			MR PRESSO test
			Intercept	P_intercept	Method	Q	Q_p val	*P* value
B cell	IgD- CD38^{br} AC	9	-0.008	0.585	MR-Egger	11.188	0.671	0.812
					IVM	12.650	0.629	
	IgD + CD38^{br} % lymphocyte	11	0.005	0.733	MR-Egger	10.172	0.337	0.354
					IVM	10.312	0.414	
	BAFF-R on B cell	13	-0.009	0.393	MR-Egger	14.536	0.205	0.326
					IVM	15.579	0.211	
Monocyte	CD14 on CD14 + CD16- monocyte	10	-0.005	0.722	MR-Egger	2.934	0.938	0.962
					IVM	3.069	0.961	
	CX3CR1 on CD14- CD16 + monocyte	11	-0.002	0.829	MR-Egger	7.184	0.618	0.617
					IVM	7.234	0.703	
T cell	CD8^{dim} %leukocyte	9	-0.004	0.933	MR-Egger	7.405	0.388	0.529
					IVM	7.413	0.493	
	CD28 + CD45RA- CD8^{dim} %CD8^{dim}	13	0.001	0.889	MR-Egger	9.590	0.568	0.668
					IVM	9.610	0.650	
	FSC-A on HLA DR + T cell	8	0.002	0.892	MR-Egger	6.084	0.414	0.568
					IVM	6.105	0.528	
Treg	CD39 + resting Treg AC	21	0.001	0.955	MR-Egger	23.500	0.216	0.264
					IVM	23.504	0.265	

Tregs (sTregs) (CD45RA-FoxP3^{lo}) [37]. The diversity of Tregs is likely a critical factor in CRC immune escape mechanisms. rTregs, which typically develop in the thymus and express low levels of FoxP3, primarily function in immune tolerance and can differentiate into aTregs with high proliferative and immunosuppressive capacity through FoxP3 upregulation. aTregs exert immune suppression in peripheral immune responses, secreting cytokines such as IL-10 and inhibiting via CTLA-4. However, they are prone to apoptosis in vitro, potentially to prevent excessive immune suppression [38]. Despite this, an increase in aTregs is associated with CRC progression and poor prognosis [39]. In contrast, sTregs express FoxP3 transiently during immune responses and may differentiate into aTregs. They exhibit strong IL-17 secretion, suggesting they may mediate immune activation and inflammation, or differentiate into Th17 cells upon appropriate stimuli [37]. sTregs secrete pro-inflammatory cytokines, such as IL-12, TNF-α, and TGF-β, creating a pro-inflammatory microenvironment potentially linked to better prognosis in CRC [40]. In addition, CD39, a key molecule expressed on Tregs, functions as a rate-limiting ectonucleotidase involved in adenosine production [41]. The CD39/CD73-adenosine axis plays a crucial role in Treg-mediated immune regulation and may facilitate CRC immune escape, consistent with our findings that CD39 + resting Tregs are a risk factor in CRC.

The interactions between Treg subsets are pivotal in CRC progression. rTregs contribute to immune tolerance and tumor immune evasion by converting into aTregs, while aTregs, in turn, regulate the expansion of rTregs through feedback mechanisms, maintaining a balance between immune tolerance and activation. sTregs, by promoting immune responses, may exert inhibitory effects on tumors, particularly in the early stages. Previous study has suggested that the conversion of sTregs to aTregs may be regulated by the upregulation of aryl hydrocarbon receptor (AHR) and its associated inhibitory factors [37]. Targeting aTregs and rTregs could potentially slow CRC progression, while modulating the immune activation capacity of sTregs may offer new strategies to counter CRC immune evasion and improve immune therapy responses.

In summary, the dynamic balance of Treg subsets and their roles in immune evasion, tumor suppression, and therapy response are critical in CRC immune regulation. A deeper understanding of the interactions among these subsets will not only elucidate the complexity of immune escape mechanisms but also provide novel therapeutic strategies for CRC immunotherapy.

Monocyte

Monocytes serve as the progenitors of macrophages and are pivotal in innate immune responses [42]. These comprise three primary subsets: the classical CD14 + CD16- monocytes, the intermediate CD14 + CD16 + monocytes, and the non-classical CD14-CD16 + monocytes [43]. The role of the CD14 receptor allows monocytes to identify and phagocytose special proteins, triggering the onset of immune reactions [44]. CD14 could enhance the capability of monocytes to recognize and respond to pathogens. Therefore, it has a protective effect in reducing the risk of CRC. Emerging research increasingly demonstrates that monocytes specifically infiltrate tumors, differentiating

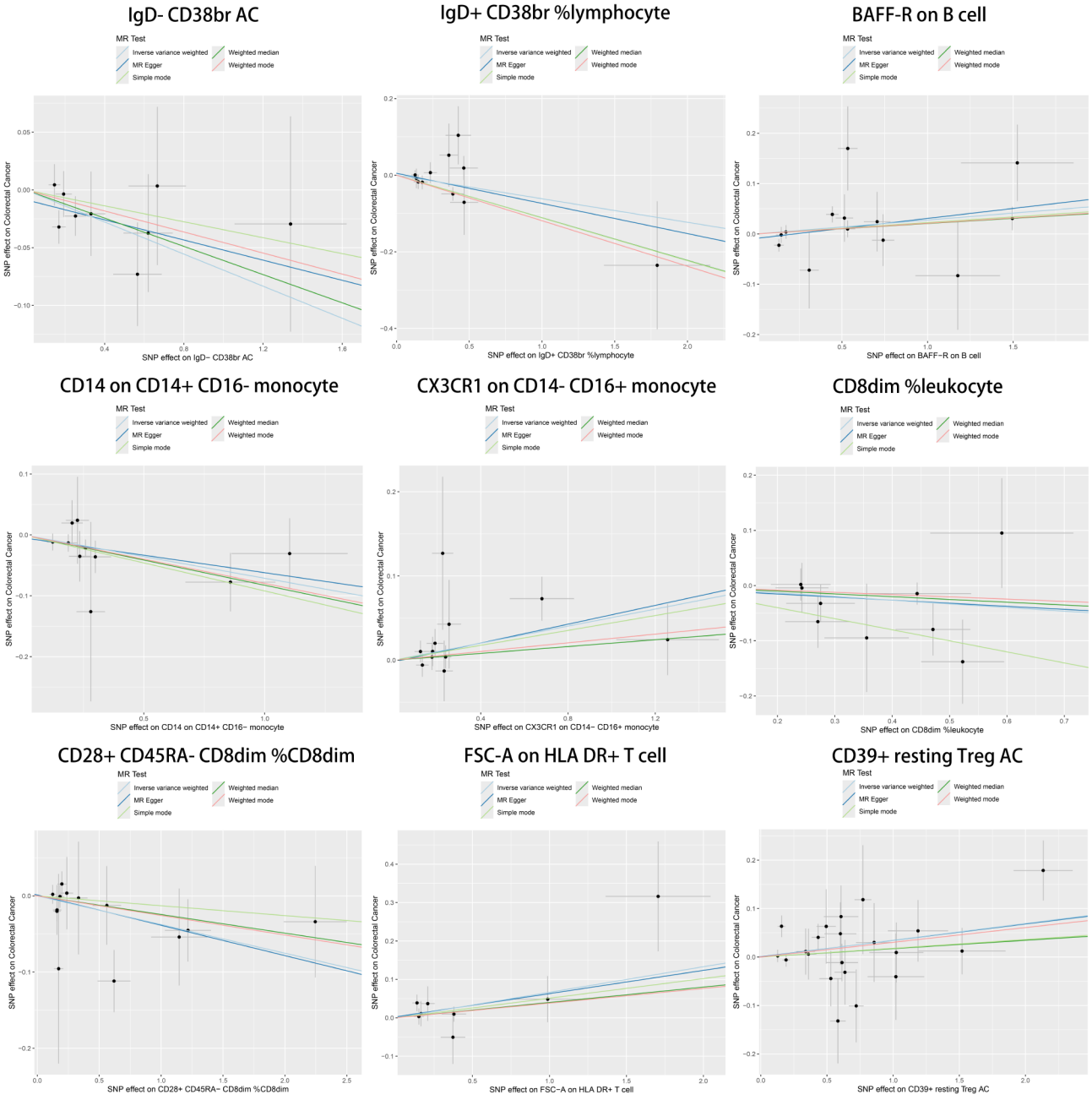

Fig. 4 Scatter plots in sensitivity analysis are employed to evaluate the causal relationship between immune phenotype and CRC risk. Each point represents the effect of a single SNP. The slope indicates the causal direction: upward for positive correlation, downward for negative correlation.The results indicate that the regression lines derived from the five MR statistical methods are generally aligned

into macrophages and congregating within unique tumor microenvironments, guided by the patterns of chemokine expression [45]. The CX3CR1/CX3CL1 receptor-ligand pair has been proven to guide monocytes to particular TME [46]. CX3CR1 is only expressed on non-classical monocytes [47], which are preferentially gathered into inflammatory TME instead of classical monocytes [48, 49]. Then they could transform into M2 macrophages by upregulating genes like Mgl2, MRC1, Fizz1, and arginase [50]. M2 macrophages have been verified to act as facilitators in promoting tumor growth in CRC [51, 52]. Targeting the CX3CR1/CX3CL1 axis could disrupt this recruitment and differentiation process, offering a potential avenue to reduce CRC risk, particularly in inflammation-driven settings.

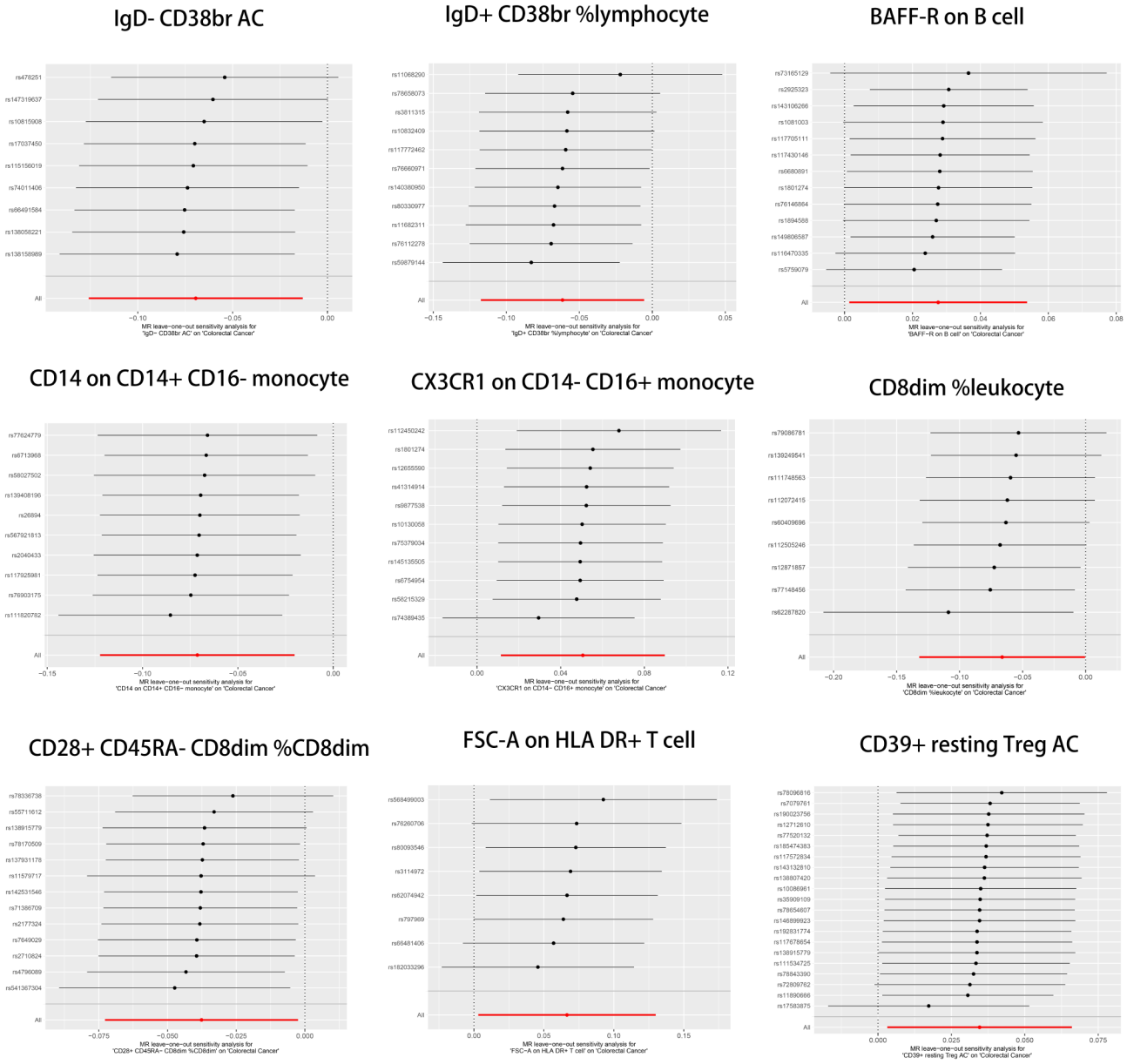

Fig. 5 Leave-one-out sensitivity analysis of nine immune cells on CRC. Each point represents the causal estimate after removing one SNP at a time, with error bars indicating the 95% confidence intervals. The red point ("All") represents the overall causal estimate using all SNPs. The results showed consistent causal estimates, indicating robust findings not driven by any single SNP

B cell

Mature B lymphocytes are categorized from Bm1 to Bm5 based on IgD and CD38 expression [53]. Among these, Bm1 (IgD + CD38–) represents virgin naïve cells, Bm2 (IgD + CD38+) are activated naïve cells, Bm2' (IgD + CD38++) are pre-germinal center (GC) cells, while Bm3 (centroblasts) and Bm4 (centrocytes), both IgD – CD38++, belong to GC cells. Bm5 (IgD – CD38+/–) comprises memory cells, which are further classified into early (CD38+) and late (CD38–) stages. Our results showed that IgD- $CD38^{br}$ (++) B cell and IgD + $CD38^{br}$ B cell were the protective factor of CRC, corresponding to GC and pre-GC cells. GCs are located in secondary lymphoid organs where lymphocytes and stromal cells gather to enhance humoral immunity [54]. Pre-GC B cells, which precede the germinal center reaction, are prepared for activation. GC B cells rapidly proliferate and mature, leading to the plasma cells-generated high-affinity antibodies and the formation of long-term memory B cells [55]. The above mechanisms are vital for developing a robust and lasting immune response against tumor antigens. Although evidence of these two cells in CRC is limited, prior research has suggested the significance of humoral immunity in cancer survival and therapy

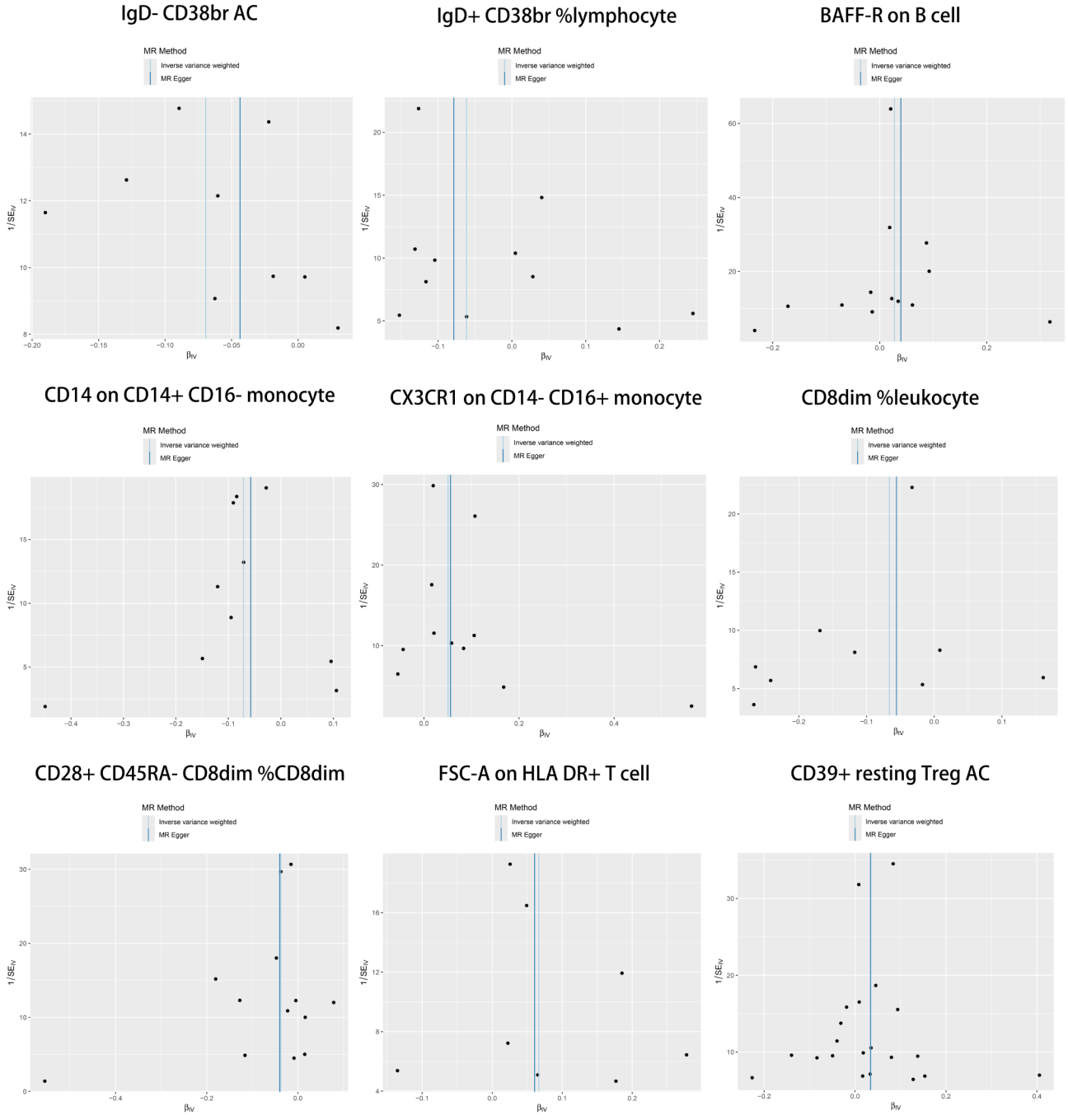

Fig. 6 Funnel plots are utilized in sensitivity analysis to evaluate the causal relationship between immune phenotypes and CRC risk. The points in the funnel plot represent the SNPs included in the study. The vertical line represents the combined OR values in the IVW and MR Egger methods

response [56–58]. The identification of IgD – $CD38^{br}$ and IgD + $CD38^{br}$ B cells as protective factors suggest their potential as biomarkers for CRC prognosis or predictors of therapy response. For instance, the activity of GC and pre-GC B cells may enhance antibody-based therapies, such as cancer vaccines or monoclonal antibody treatments, by boosting humoral immunity against tumor-specific antigens.

BAFF-R

B cell-activating factor receptor (BAFF-R) is primarily expressed in all B cells [59, 60], where it firmly binds to BAFF, a crucial maturation factor for B cells [61]. Current insights posit BAFF as critical contributors to the pathology of solid tumors. Elevated levels of BAFF and BAFF-R have been identified across various cancers, showing correlations with tumor progression and treatment efficacy [62–64]. In frozen CRC tissues, An et al. [65]found the

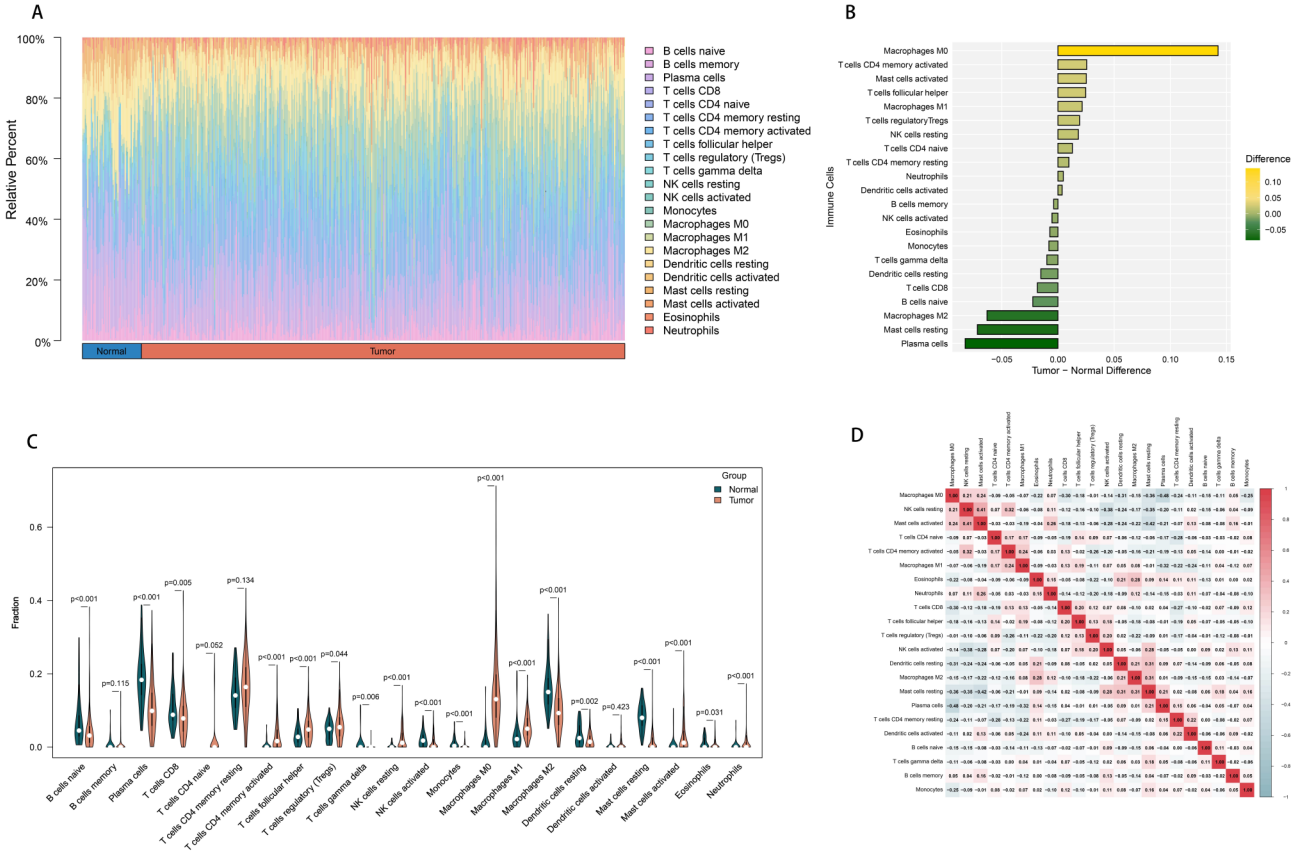

Fig. 7 Composition of infiltrated immune cells between paired tumor and adjacent normal tissues in the TCGA cohort with CIBERSORT $p < 0.05$. **(A)** Fractions of immune cells in 400 tumor and 49 normal samples in TCGA. **(B)** Comparisons of immune cells more in tumor and more in normal tissues in TCGA. Left bars show immune cells enriched in normal tissues, right bars show immune cells enriched in tumor tissues. Darker colors indicate higher proportions. **(C)** The violin plot shows the distribution of immune cell infiltration in tumor (orange) and normal (green) tissues. White dots represent medians and p-values indicate statistical significance between groups. **(D)** The correlation heatmap showing pairwise correlations between immune cell types. Red indicates positive correlations, blue indicates negative correlations, with color intensity reflecting correlation strength

concentration of BAFF was significantly high. Besides, Chereches et al. detected BAFF level in metastatic CRC (mCRC) patients received chemotherapy. The results showed high BAFF level was a risk factor for survival (2-year OS 63 vs. 32%, $p < 0.01$; 2-year PFS 50 vs. 29%, $p < 0.05$) [66]. Currently, BAFF targeted therapies [67] (belimumab and tabalumab) and BAFF-R targeted therapies (VAY-736) have been primarily conducted clinical trials in hematologic tumors, such as multiple myeloma (MM) [68] and chronic lymphocytic leukemia (CLL) [69]. These therapies have shown promise in modulating BAFF/BAFF-R-mediated pathways, suggesting potential applicability in solid tumors, including CRC. Future studies should focus on understanding the dynamic role of BAFF in CRC progression and immune modulation, as well as validating BAFF-targeted therapies in preclinical and clinical CRC models. These investigations could pave the way for developing novel, personalized therapeutic strategies targeting BAFF in CRC.

Our results did not find the inverse causal relationship between CRC and immune phenotypes, which might be attributed to the temporal window of causality. Changes in immune phenotypes may result from CRC progression in later stages, rather than a cause in the early stages. MR analysis assumes a linear causal relationship and stable effects between genetic instruments and outcomes. However, the dynamic interaction between cancer and the immune system may not be fully captured by MR analysis. In early-stage CRC, the immune system exhibits robust tumor surveillance and elimination abilities. It can identify mutated or cancer-specific antigens, initiating immune responses that target and eliminate potential CRC cells [70]. During this stage, there is marked local immune activation, characterized by substantial infiltration of CD8 + T cells around the tumor, along with a dense presence of cDCs in the tumor-associated lymph nodes [71]. As CRC progresses, the tumor may adopt various immune evasion strategies, such as upregulation of immune checkpoint like PD-L1/PD-1, recruitment of immunosuppressive cells (e.g., Tregs and MDSCs), and downregulation of MHC molecules [70]. Immune cells undergo a shift from an anti-tumor phenotype to an

immunosuppressive phenotype, or the dysfunction of T cells and antigen-presenting cells contribute to tumor immune escape. Studies have demonstrated that in late-stage CRC, Tregs significantly accumulate in the lymph nodes, exhibiting elevated expression of FoxP3 and IL-10 [72]. These cytokines suppress the differentiation and maturation of cDCs, reducing their numbers and thereby aiding tumor immune evasion [73]. Moreover, metastatic CRC tissues show a marked increase in MDSCs and a reduction in NK cells compared to adjacent normal tissues [74]. Elevated MDSCs inhibit T cell proliferation, promote Treg development, and contribute to the enhancement of immune suppression within the TME.

The dynamic transition from immune activation in early-stage CRC to immune evasion in late-stage CRC highlights the complexity of the immune landscape during tumor progression. This does not imply that immune phenotype changes are a direct result of tumor initiation. Instead, immune phenotype changes are likely adaptive responses during tumor development, not the starting point of a reverse causal chain. This hypothesis highlights the complex bidirectional relationship between cancer and the immune system. Future studies integrating longitudinal data and multi-omics analyses will be crucial to further explore the dynamic immune responses and underlying mechanisms during CRC progression.

Our research explores the causality between immune cell phenotypes and CRC using MR methods. The results reduce the interference of confounding variables, derived through rigorous assessment of horizontal pleiotropy and reverse causality. Besides, the immunophenotypes we found have been less identified in prior studies. Our study still has some limitations. Firstly, given the scarcity of GWAS studies on immune cells and the lack of detailed clinical data on immune cell infiltration, we could not correlate immune cells with the polygenic risk score (PRS) constructed for CRC. Secondly, performing multivariable MR is not feasible based on the complexities, including the effectiveness of IVs, statistical power, and computational demands from 731 immune exposures. More advances in methodology could be instrumental in refining the accuracy of our analysis.

Focus on immune cells in CRC holds profound implications for clinical practice and future research, guiding the advancement of target immunotherapy and novel treatment strategies. Specific immunophenotypes, like IgD- CD38br and IgD + CD38br B cell, CD8dim and CD28 + CD45RA- CD8dim T cells, CD39 + resting Treg, BAFF-R on B cell, CD14 and CX3CR1 on monocyte, could become predictive and prognostic biomarkers in the future studies. It could be a new trend exploring the dynamic changes of immune cells throughout the tumor progression. According to the specific immune profiles, patients could receive more precise and individual therapies.

Conclusion

Utilizing Mendelian randomization analysis, our research has illuminated the causal links between specific immune cell traits and colorectal cancer, revealing the intricate cross-talk between the immune TME and the disease. These insights expand our understanding of immunological factors in colorectal cancer and provide important clues for its prevention. They may also facilitate earlier diagnosis and encourage more effective therapeutic strategies.

Supplementary Information

The online version contains supplementary material available at https://doi.org/10.1186/s12885-025-13576-4 .

Supplementary Material 1: Supplementary Table 1: The association between all SNPs and immune cells. Supplementary Table 2: Qualified instrumental variables for MR analysis of immune cells and CRC. Supplementary Table 3: Nine immune immunophenotypes were positively linked to the risk of CRC. Supplementary Table 4: Reverse MR between CRC and immunophenotypes. Supplementary Table 5: SNPs from the UK Biobank used for MR analysis. Supplementary Table 6: SNPs from the FinnGen cohorts used for MR analysis. Supplementary Table 7: MR analysis between immune cells and CRC in the UK Biobank database. Supplementary Table 8: MR analysis between immune cells and CRC in the FinnGen cohorts. Supplementary Table 9: Composition of infiltrated immune cells between paired tumor ($n = 400$) and adjacent normal tissues ($n = 49$) in the TCGA cohort after CIBERSORT P value filtration

Acknowledgements

None.

Author contributions

LST and RZL designed the research plan for this study. LRZ and LST completed the manuscript writing. LST, YJL, and HDH completed the image processing and data statistical analysis. JYL revised the manuscript. All the authors approved the final version of the manuscript.

Funding

The author(s) declare financial support was received for the research, authorship, and/or publication of this article. This study was supported by the Sichuan Science and Technology Department Key Research and Development Project (2019YFS0539), 1.3.5 Project for Disciplines of Excellence, West China Hospital, Sichuan University (ZYJC18022 and ZYJC21017) and the National Clinical Research Center for Geriatrics (West China Hospital, Z2018B12).

Data availability

Data is provided within the manuscript or supplementary information files. GWAS summary statistics for each immune cell are publicly available from the GWAS Catalog (accession numbers from GCST0001391 to GCST0002121) and CRC related GWAS data can be got from IEU (https://gwas.mrcieu.ac.uk/).

Declarations

Ethics approval and consent to participate

According to guidance received from our research ethics board, no ethics review is required for studies utilizing public data sets.

Consent for publication

Not applicable.

Competing interests
The authors declare no competing interests.

Author details
[1]School of Medical and Life Sciences, Chengdu University of Traditional Chinese Medicine, Chengdu, China
[2]Department of Biotherapy, Cancer Center, West China Hospital of Sichuan University, 37 Guoxue Xiang Street, Chengdu, Sichuan Province 610041, China
[3]Mental Health Center and Psychiatric Laboratory, The State Key Laboratory of Biotherapy, West China Hospital of Sichuan University, Chengdu, Sichuan, China
[4]Queen Mary College, Nanchang University, Nanchang, Jiangxi, China

Received: 24 April 2024 / Accepted: 21 January 2025
Published online: 03 March 2025

References

1. Siegel RL, et al. Cancer statistics, 2024. CA Cancer J Clin. 2024;74(1):12–49.
2. Chambers AC, et al. Demographic trends in the incidence of young-onset colorectal cancer: a population-based study. Br J Surg. 2020;107(5):595–605.
3. Hull MA. Nutritional prevention of colorectal cancer. Proc Nutr Soc. 2021;80(1):59–64.
4. Li SKH, et al. Mismatch repair and Colon cancer: mechanisms and therapies explored. Trends Mol Med. 2016;22(4):274–89.
5. André T, et al. Pembrolizumab in microsatellite-instability-high Advanced Colorectal Cancer. N Engl J Med. 2020;383(23):2207–18.
6. Overman MJ, et al. Durable clinical benefit with Nivolumab Plus Ipilimumab in DNA mismatch Repair-Deficient/Microsatellite instability-high metastatic colorectal Cancer. J Clin Oncol. 2018;36(8):773–9.
7. Hiam-Galvez KJ, et al. Systemic immunity in cancer. Nat Rev Cancer. 2021;21(6):345–59.
8. Tang T, et al. Advantages of targeting the tumor immune microenvironment over blocking immune checkpoint in cancer immunotherapy. Signal Transduct Target Ther. 2021;6(1):72.
9. Zheng Z et al. T cells in Colorectal Cancer: unravelling the function of different T cell subsets in the Tumor Microenvironment. Int J Mol Sci 2023;24(14).
10. Pagès F, et al. In situ cytotoxic and memory T cells predict outcome in patients with early-stage colorectal cancer. J Clin Oncol. 2009;27(35):5944–51.
11. Myers JA, et al. Exploring the NK cell platform for cancer immunotherapy. Nat Rev Clin Oncol. 2021;18(2):85–100.
12. Pietropaolo G, et al. NK cell and ILC heterogeneity in colorectal cancer. New perspectives from high dimensional data. Mol Aspects Med. 2021;80:100967.
13. Ward-Hartstonge KA, et al. Regulatory T-cell heterogeneity and the cancer immune response. Clin Transl Immunol. 2017;6(9):e154.
14. Song M, et al. Systemic Immune Response and Cancer Risk: filling the Missing Piece of Immuno-Oncology. Cancer Res. 2020;80(9):1801–3.
15. Vlad C, et al. The prognostic value of FOXP3 + T regulatory cells in colorectal cancer. J buon. 2015;20(1):114–9.
16. Qian J, et al. A pan-cancer blueprint of the heterogeneous tumor microenvironment revealed by single-cell profiling. Cell Res. 2020;30(9):745–62.
17. Zhang JP, et al. Action of circulating and infiltrating B cells in the immune microenvironment of colorectal cancer by single-cell sequencing analysis. World J Gastrointest Oncol. 2024;16(6):2683–96.
18. Bindea G, et al. Spatiotemporal dynamics of intratumoral immune cells reveal the immune landscape in human cancer. Immunity. 2013;39(4):782–95.
19. Thorsson V, et al. The Immune Landscape of Cancer. Immunity. 2018;48(4):812–e830814.
20. O'Keefe SJ. Diet, microorganisms and their metabolites, and colon cancer. Nat Rev Gastroenterol Hepatol. 2016;13(12):691–706.
21. Smith GD, et al. Mendelian randomization': can genetic epidemiology contribute to understanding environmental determinants of disease? Int J Epidemiol. 2003;32(1):1–22.
22. Orrù V, et al. Complex genetic signatures in immune cells underlie autoimmunity and inform therapy. Nat Genet. 2020;52(10):1036–45.
23. McKay JD, et al. Large-scale association analysis identifies new lung cancer susceptibility loci and heterogeneity in genetic susceptibility across histological subtypes. Nat Genet. 2017;49(7):1126–32.
24. Sakaue S, et al. A cross-population atlas of genetic associations for 220 human phenotypes. Nat Genet. 2021;53(10):1415–24.
25. Burrows K et al. Genome-wide Association study of Cancer Risk in UK Biobank. 2021; https://doi.org/10.5523/bris.aed0u12w0ede20olb0m77p4b9
26. Nieuwkamp DJ, et al. Changes in case fatality of aneurysmal subarachnoid haemorrhage over time, according to age, sex, and region: a meta-analysis. Lancet Neurol. 2009;8(7):635–42.
27. Pierce BL, et al. Power and instrument strength requirements for mendelian randomization studies using multiple genetic variants. Int J Epidemiol. 2011;40(3):740–52.
28. Burgess S, et al. Avoiding bias from weak instruments in mendelian randomization studies. Int J Epidemiol. 2011;40(3):755–64.
29. Hemani G et al. The MR-Base platform supports systematic causal inference across the human phenome. Elife 2018;7.
30. Burgess S, et al. A review of instrumental variable estimators for mendelian randomization. Stat Methods Med Res. 2017;26(5):2333–55.
31. Burgess S, et al. Sensitivity analyses for robust causal inference from mendelian randomization analyses with multiple genetic variants. Epidemiology. 2017;28(1):30–42.
32. Newman AM, et al. Robust enumeration of cell subsets from tissue expression profiles. Nat Methods. 2015;12(5):453–7.
33. Kumari S, et al. CD8(dim) but not CD8(bright) cells positive to CD56 dominantly express KIR and are cytotoxic during visceral leishmaniasis. Hum Immunol. 2018;79(8):616–20.
34. Esensten JH, et al. CD28 Costimulation: from mechanism to Therapy. Immunity. 2016;44(5):973–88.
35. Meraviglia S, et al. T-Cell subsets (T(CM), T(EM), T(EMRA)) and polyfunctional Immune response in patients with human immunodeficiency virus (HIV) infection and different T-CD4 cell response. Ann Clin Lab Sci. 2019;49(4):519–28.
36. Toma G, et al. Transcriptional analysis of total CD8(+) T cells and CD8(+) CD45RA(-) memory T cells from Young and Old Healthy Blood donors. Front Immunol. 2022;13:806906.
37. Miyara M, et al. Functional delineation and differentiation dynamics of human CD4 + T cells expressing the FoxP3 transcription factor. Immunity. 2009;30(6):899–911.
38. Xin L, et al. Increased pro-inflammatory cytokine-secreting regulatory T cells are correlated with the plasticity of T helper cell differentiation and reflect disease status in asthma. Respir Med. 2018;143:129–38.
39. Aristin Revilla S, et al. Colorectal Cancer-Infiltrating Regulatory T Cells: functional heterogeneity, metabolic adaptation, and therapeutic targeting. Front Immunol. 2022;13:903564.
40. Saito T, et al. Two FOXP3(+)CD4(+) T cell subpopulations distinctly control the prognosis of colorectal cancers. Nat Med. 2016;22(6):679–84.
41. Dwyer KM, et al. CD39 and control of cellular immune responses. Purinergic Signal. 2007;3(1–2):171–80.
42. Ley K, et al. Monocyte and macrophage dynamics during atherogenesis. Arterioscler Thromb Vasc Biol. 2011;31(7):1506–16.
43. Lee HW, et al. Recruitment of monocytes/macrophages in different tumor microenvironments. Biochim Biophys Acta. 2013;1835(2):170–9.
44. Devitt A, et al. Human CD14 mediates recognition and phagocytosis of apoptotic cells. Nature. 1998;392(6675):505–9.
45. Murdoch C, et al. The role of myeloid cells in the promotion of tumour angiogenesis. Nat Rev Cancer. 2008;8(8):618–31.
46. Murdoch C, et al. Mechanisms regulating the recruitment of macrophages into hypoxic areas of tumors and other ischemic tissues. Blood. 2004;104(8):2224–34.
47. Gevrey JC, et al. Syk is required for monocyte/macrophage chemotaxis to CX3CL1 (Fractalkine). J Immunol. 2005;175(6):3737–45.
48. Auffray C, et al. Blood monocytes: development, heterogeneity, and relationship with dendritic cells. Annu Rev Immunol. 2009;27:669–92.
49. Qian BZ, et al. CCL2 recruits inflammatory monocytes to facilitate breast-tumour metastasis. Nature. 2011;475(7355):222–5.
50. Pucci F, et al. A distinguishing gene signature shared by tumor-infiltrating Tie2-expressing monocytes, blood resident monocytes, and embryonic macrophages suggests common functions and developmental relationships. Blood. 2009;114(4):901–14.
51. Zhang M, et al. Roles of macrophages on ulcerative colitis and colitis-associated colorectal cancer. Front Immunol. 2023;14:1103617.
52. Zhao S, et al. Tumor-derived exosomal miR-934 induces macrophage M2 polarization to promote liver metastasis of colorectal cancer. J Hematol Oncol. 2020;13(1):156.
53. Sanz I, et al. Phenotypic and functional heterogeneity of human memory B cells. Semin Immunol. 2008;20(1):67–82.

54. Victora GD, et al. Germinal centers. Annu Rev Immunol. 2022;40:413–42.
55. Tarlinton D. B-cell memory: are subsets necessary? Nat Rev Immunol. 2006;6(10):785–90.
56. Lin HH, et al. Phytogalactolipids activate humoral immunity against colorectal cancer. J Exp Clin Cancer Res. 2023;42(1):95.
57. Bohne A, et al. Impact of laparoscopic versus open surgery on humoral immunity in patients with colorectal cancer: a systematic review and meta-analysis. Surg Endosc. 2024;38(2):540–53.
58. Wang SS, et al. Tumor-infiltrating B cells: their role and application in anti-tumor immunity in lung cancer. Cell Mol Immunol. 2019;16(1):6–18.
59. Vincent FB, et al. The BAFF/APRIL system: emerging functions beyond B cell biology and autoimmunity. Cytokine Growth Factor Rev. 2013;24(3):203–15.
60. Thompson JS, et al. BAFF-R, a newly identified TNF receptor that specifically interacts with BAFF. Science. 2001;293(5537):2108–11.
61. Schneider P, et al. BAFF, a novel ligand of the tumor necrosis factor family, stimulates B cell growth. J Exp Med. 1999;189(11):1747–56.
62. Jablonska E, et al. Overexpression of B cell-activating factor (BAFF) in neutrophils of oral cavity cancer patients - preliminary study. Neoplasma. 2011;58(3):211–6.
63. Pelekanou V, et al. BCMA (TNFRSF17) induces APRIL and BAFF mediated breast Cancer Cell Stemness. Front Oncol. 2018;8:301.
64. Fragioudaki M, et al. Serum BAFF levels are related to angiogenesis and prognosis in patients with multiple myeloma. Leuk Res. 2012;36(8):1004–8.
65. An S et al. Expression of Immune-related and inflammatory markers and their prognostic impact in Colorectal Cancer patients. Int J Mol Sci 2023;24(14).
66. Chereches G, et al. Biomarkers for the early detection of relapses in metastatic colorectal cancers. J buon. 2017;22(3):658–66.
67. McWilliams EM, et al. Anti-BAFF-R antibody VAY-736 demonstrates promising preclinical activity in CLL and enhances effectiveness of ibrutinib. Blood Adv. 2019;3(3):447–60.
68. Raje NS, et al. Phase 1 study of Tabalumab, a human Anti-B-Cell activating factor antibody, and Bortezomib in patients with Relapsed/Refractory multiple myeloma. Clin Cancer Res. 2016;22(23):5688–95.
69. Tandler C et al. Neutralization of B-Cell activating factor (BAFF) by Belimumab reinforces small molecule inhibitor treatment in chronic lymphocytic leukemia. Cancers (Basel). 2020;12(10).
70. Dunn GP, et al. Cancer immunoediting: from immunosurveillance to tumor escape. Nat Immunol. 2002;3(11):991–8.
71. Guo L, et al. Colorectal Cancer Immune infiltrates: significance in patient prognosis and immunotherapeutic efficacy. Front Immunol. 2020;11:1052.
72. Olguín JE, et al. Early and partial reduction in CD4(+)Foxp3(+) Regulatory T cells during colitis-Associated Colon Cancer induces CD4(+) and CD8(+) T cell activation inhibiting Tumorigenesis. J Cancer. 2018;9(2):239–49.
73. Sánchez-Paulete AR, et al. Antigen cross-presentation and T-cell cross-priming in cancer immunology and immunotherapy. Ann Oncol. 2017;28(suppl12):xii74.
74. Chen Y, et al. The role of the Tumor Microenvironment and Treatment Strategies in Colorectal Cancer. Front Immunol. 2021;12:792691.

Publisher's note